nature | methods

Cell stimulation with optically manipulated microsources

Holger Kress, Jin-Gyu Park, Cecile O Mejean, Jason D Forster, Jason Park, Spencer S Walse, Yong Zhang, Dianqing Wu, Orion D Weiner, Tarek M Fahmy & Eric R Dufresne

Supplementary figures and text:

Note: Supplementary Videos 1–8 are available on the Nature Methods website.

Supplementary Figure 1

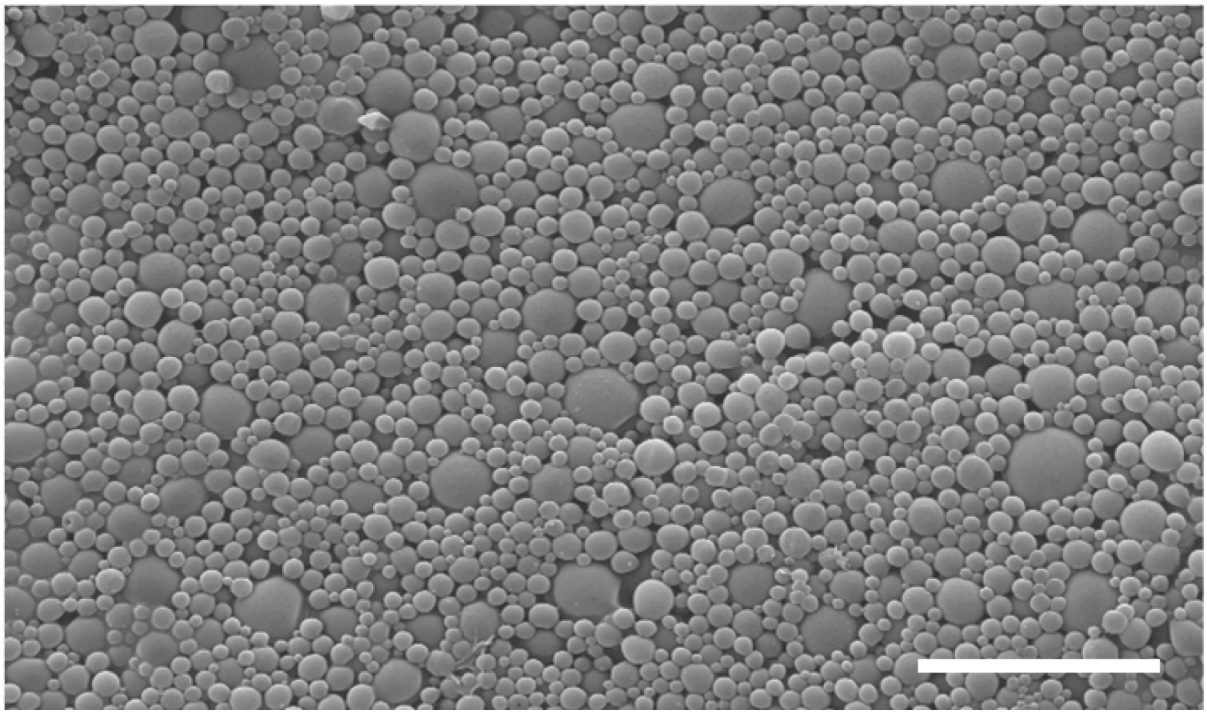

Supplementary Figure 1 | Structure of the controlled-release microparticles. Scanning electron micrograph of fMLP-loaded PLGA microparticles. The diameters of the particles shown here range from 200 nm to 2 µm. The average diameter is 500 nm and the polydispersity (standard deviation of diameter divided by mean diameter) is 40%. Scale bar: 5 µm.

Nature Methods: doi:10.1038/nmeth.1400

Supplementary Figure 2

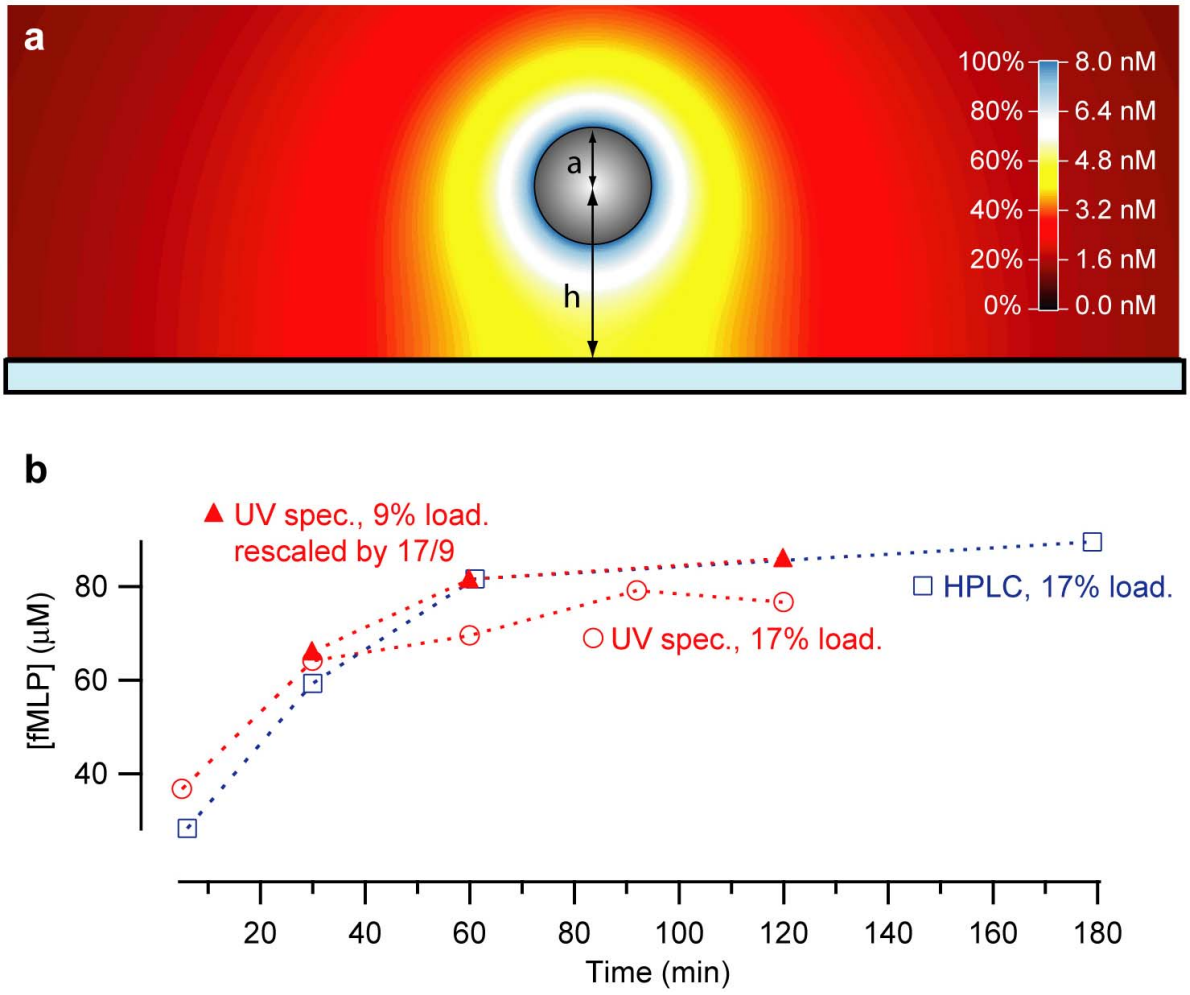

Supplementary Figure 2 | Release characteristics of the chemoattractant-loaded microparticles. (**a**) Calculated concentration of chemoattractant around an individual microparticle (*a*: radius of particle, *h*: height of particle position above coverslip). The plane shown here is perpendicular to the coverslip plane and goes through the center of the bead. The scale bar is labeled with relative concentrations (where 100% is the maximal concentration on the surface of the bead) and with absolute concentrations. The absolute concentrations were calculated for a bead with 17% nominal loading and a diameter of 2 µm. (**b**) HPLC and UV fluorescence spectroscopy (UV spec.) measurements of the cumulative concentration of fMLP released from PLGA microparticles at a microparticle concentration of 1 mg/ml. Two of the curves show data from beads with a higher nominal loading (17%) and one curve shows data from beads with a lower loading (9%). The curve for the lower loading was rescaled with a factor 17/9 to make the curves comparable.

Nature Methods: doi:10.1038/nmeth.1400

Supplementary Figure 3

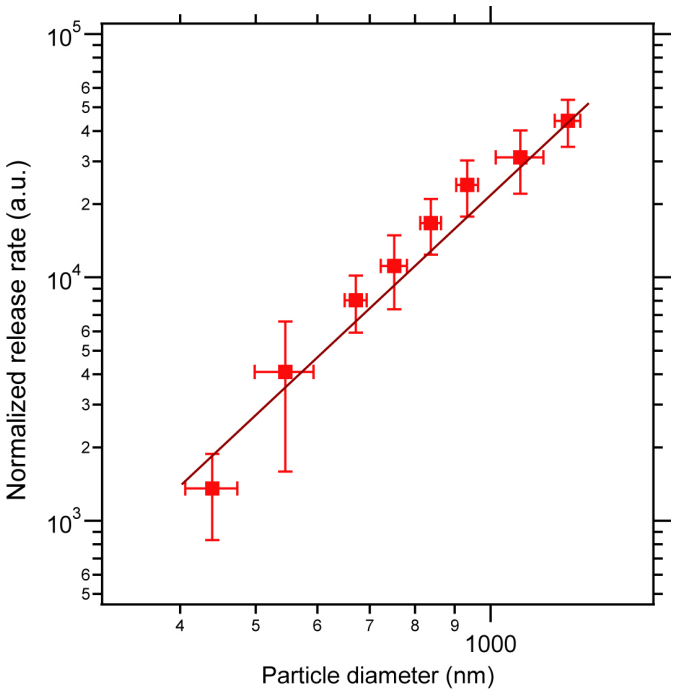

Supplementary Figure 3 | Particle size dependence of release rate. Shown are the mean values and the standard deviations of the normalized release rate (which is proportional to the number of molecules released per time interval) as a function of the bead diameter. The solid line has a slope of 3 in the double-logarithmic plot. The release rate scales approximately with the volume of the particle.

Nature Methods: doi:10.1038/nmeth.1400

Supplementary Figure 4

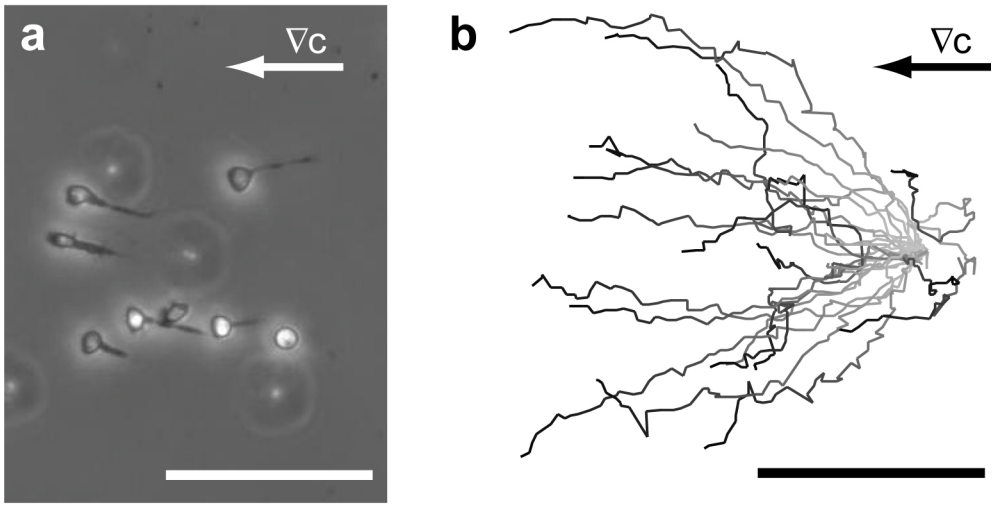

Supplementary Figure 4 | Chemoattractant released from beads is able to induce neutrophil migration in a gradient chamber. Migration of HL60 neutrophils in a Zigmond gradient chamber filled on the left side with fMLP released from PLGA beads and on the right side with control buffer. The arrows in both panels indicate the direction of the gradient ∇c . (**a**) Phase contrast image of migrating HL60 cells in the chamber. (**b**) Cell tracking analysis: Trajectories of 27 cells in the image plane over the time course of 30 minutes. The trajectories were displaced to start at the same location. The gray values of the trajectories indicate the time: light gray = start of trajectory, black = end of trajectory. Scale bars: 100 µm.

Nature Methods: doi:10.1038/nmeth.1400

Supplementary Figure 5

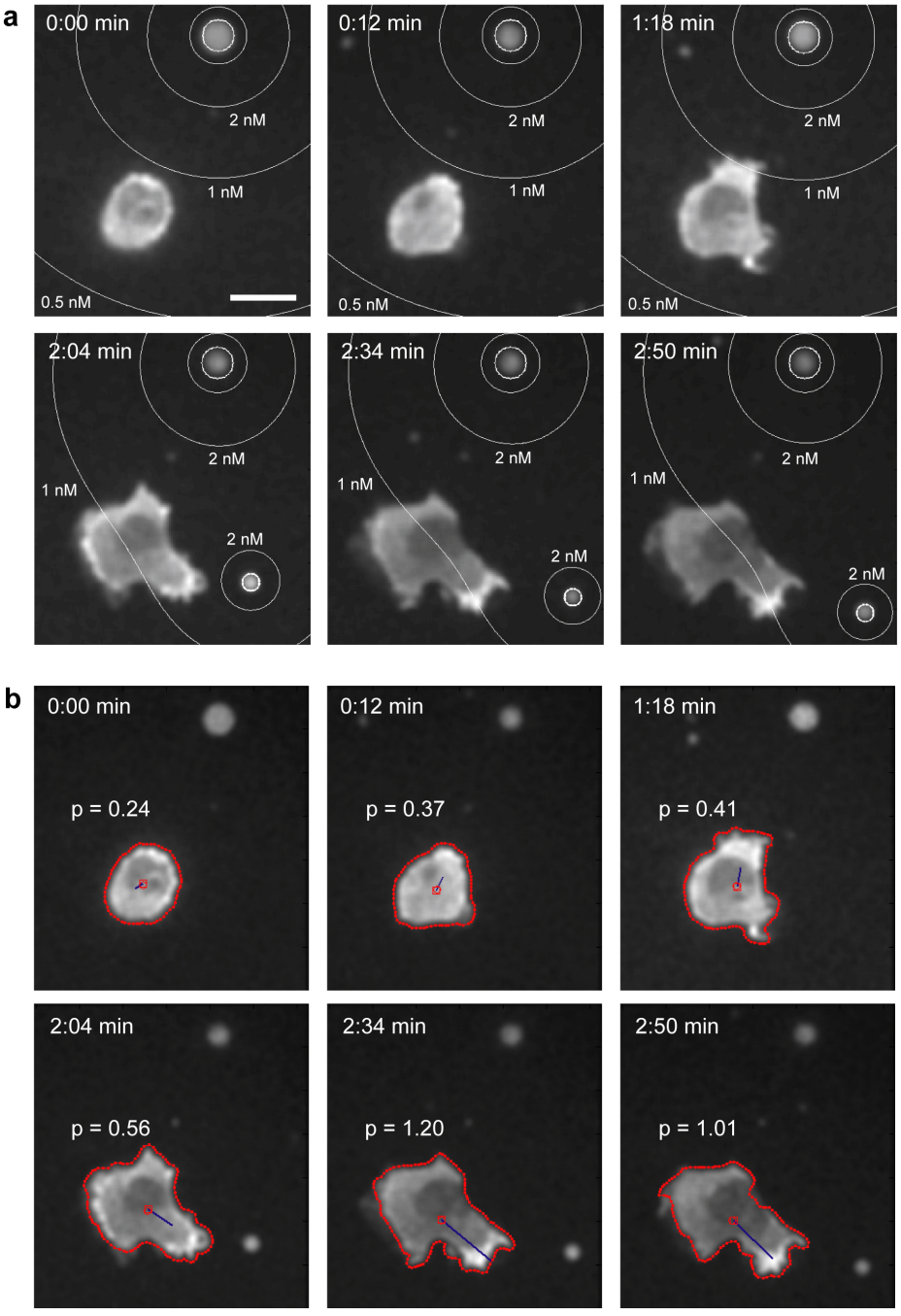

Supplementary Figure 5 | Microsources of chemoattractant induce changes in the intracellular actin distribution. Time lapse image series (spinning disk confocal microscopy) of a neutrophil-differentiated HL-60 cell transiently transfected with YFP-actin in a suspension of beads releasing the chemoattractant fMLP. (**a**) The contour lines show the calculated concentration of fMLP released from the beads on top of a homogeneous background concentration. (**b**) The cell polarization analysis shows the direction of the polarization and the strength *p* of the polarization. Scale bar: 10 µm.

Nature Methods: doi:10.1038/nmeth.1400

Supplementary Figure 6

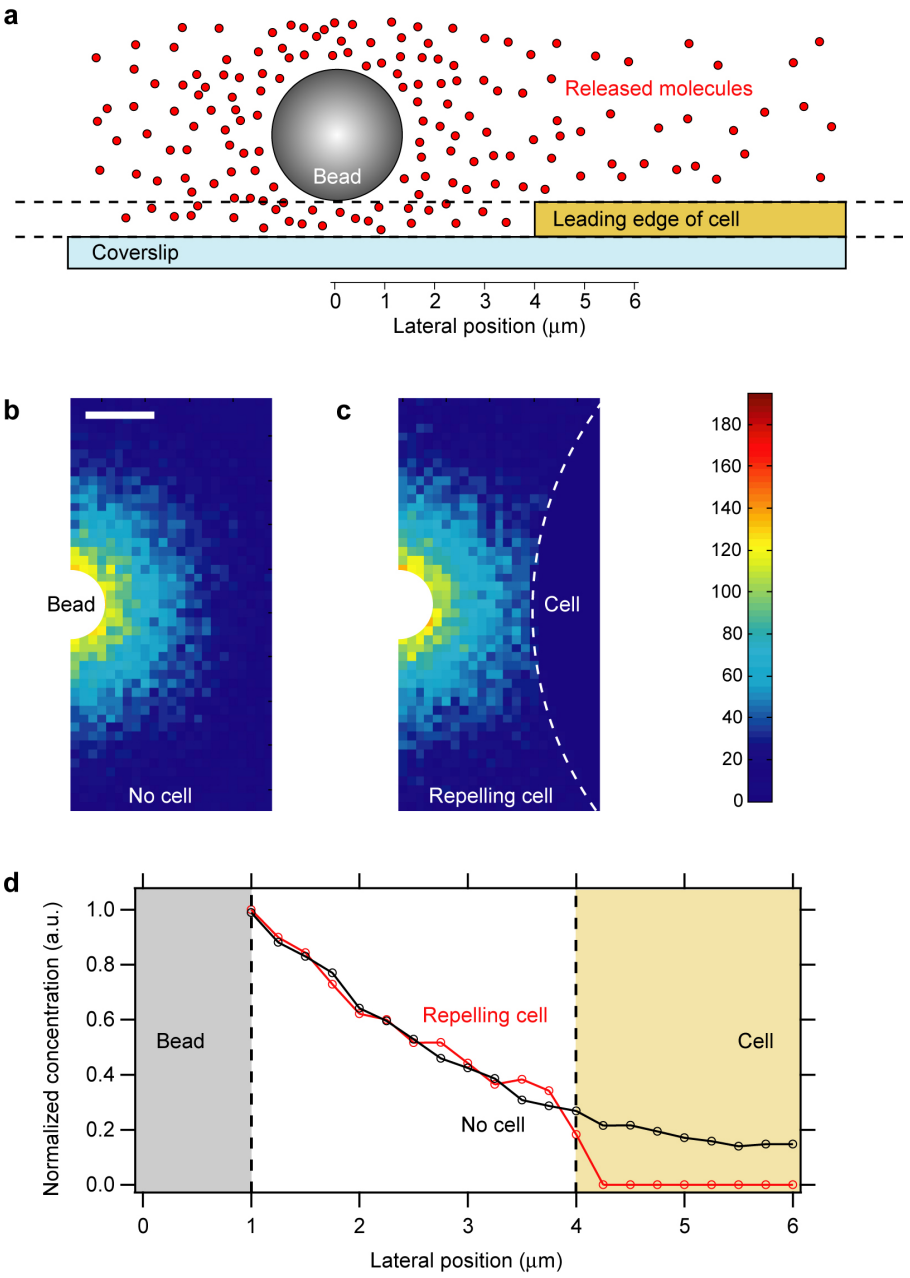

Supplementary Figure 6 | Influence of a cell on the concentration pattern around a microsource. (**a**) Schematic side view (xz-plane) of the 3D stochastic simulation of a bead releasing diffusing molecules in vicinity to a leading edge of a cell. (**b, c**) 2D concentration distributions (xy-plane) around the microsource (on the left side of each image) in the absence of a cell and in the presence of a repelling cell (on the right side of the image). The position (directly above the coverslip) and thickness (0.5 µm) of the slices shown in **b** and **c** are indicated by the dashed lines in panel **a**. Scale bar: 2 µm. (**d**) Horizontal line profiles of the concentration distributions show that the concentration profile between bead and cell is not affected significantly by the presence of the cell.

Nature Methods: doi:10.1038/nmeth.1400

Supplementary Figure 7

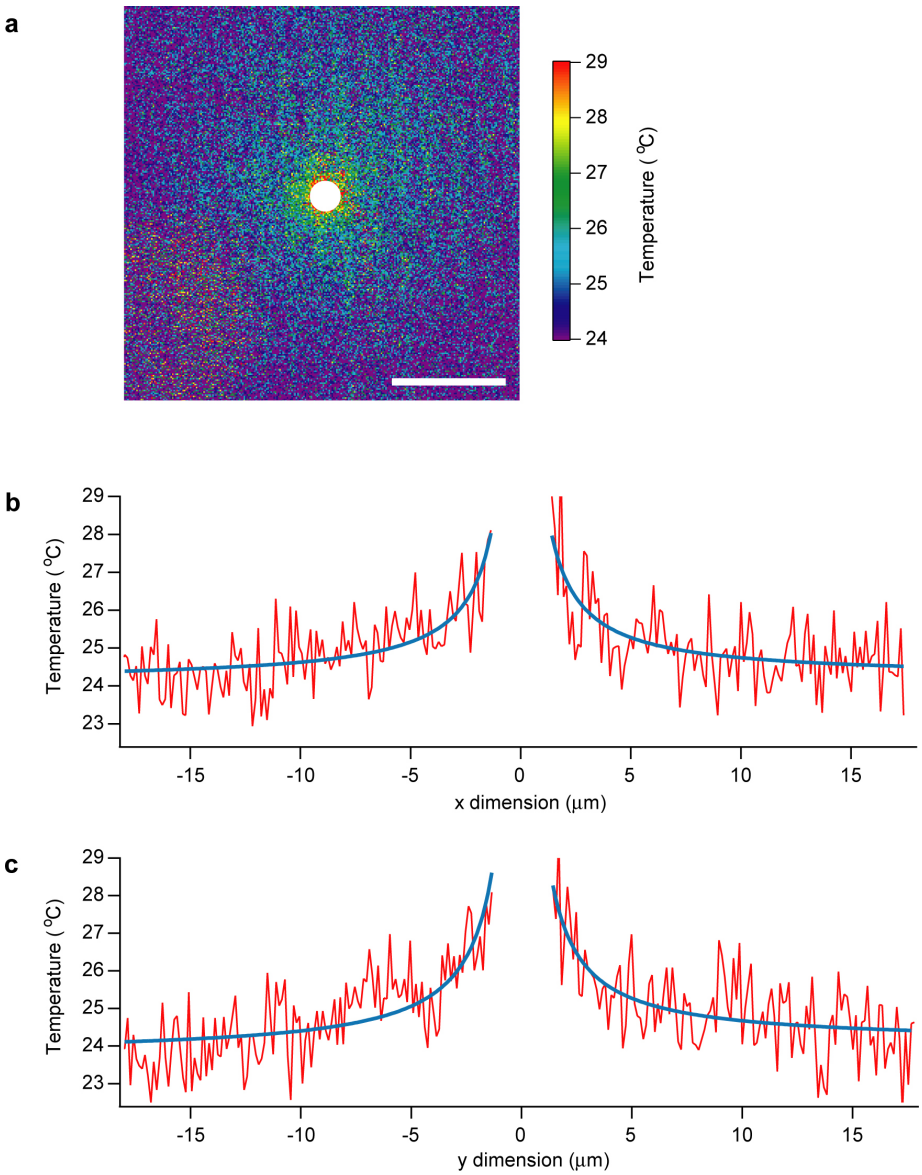

Supplementary Figure 7 | Heating of a bead in a high power optical trap. (**a**) Temperature distribution around a bead in a trap at a laser power of about 230 mW in the focal plane. (**b, c**) Line profiles through the center of the temperature distribution in x- and y-direction.

Nature Methods: doi:10.1038/nmeth.1400

Supplementary Figure 8

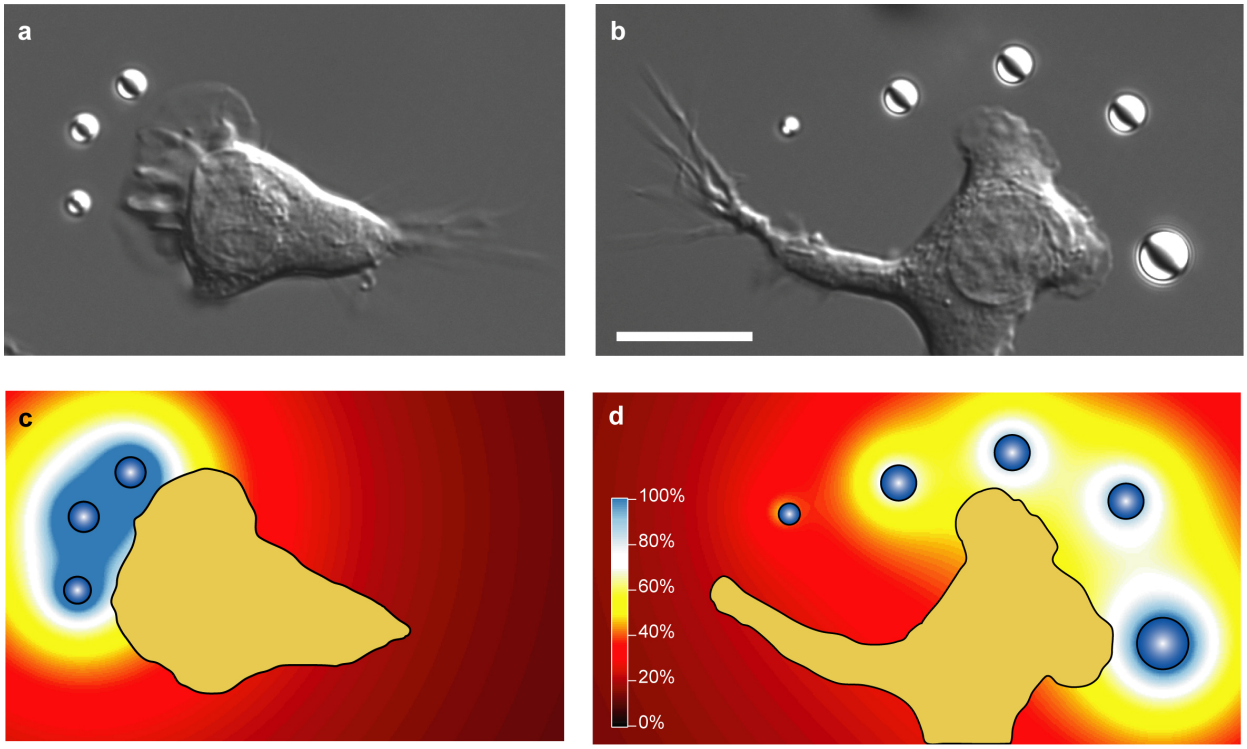

Supplementary Figure 8 | Spatially flexible cell stimulation with optically manipulated microsources. (**a, b**) DIC images of polarized HL-60 neutrophils with multiple optically trapped PLGA beads loaded with the chemoattractant fMLP. Scale bar: 10 µm. (**c, d**) Calculated concentration distribution of fMLP released from the beads.

Nature Methods: doi:10.1038/nmeth.1400

Supplementary Figure 9

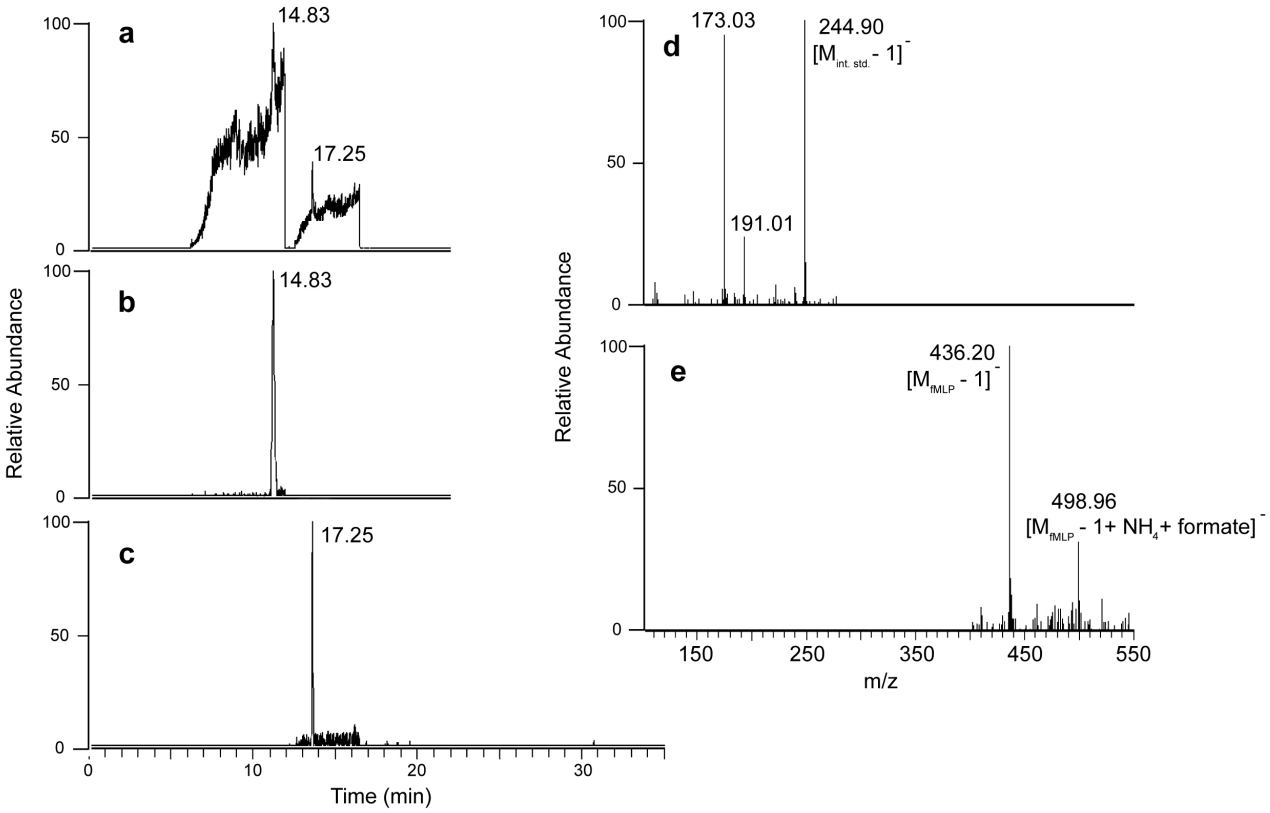

Supplementary Figure 9 | HPLC detection of fMLP released from PLGA beads. HPLC-MS (-) ESI of an aliquot from the fMLP (MW 437) matrix with an added internal standard (MW 246). (**a**) Total ion current (TIC) over scan segments *m/z* 100-275 (10-15min) and *m/z* 400-550 (16-21min); TIC ion-extraction of *m/z* 245 ± 0.5 (**b**) and *m/z* 436 ± 0.5; 499 ± 0.5 (**c**). Mass spectra that correspond to ion trace B (**d**) and trace C (**e**).

Nature Methods: doi:10.1038/nmeth.1400

Supplementary Figure 10

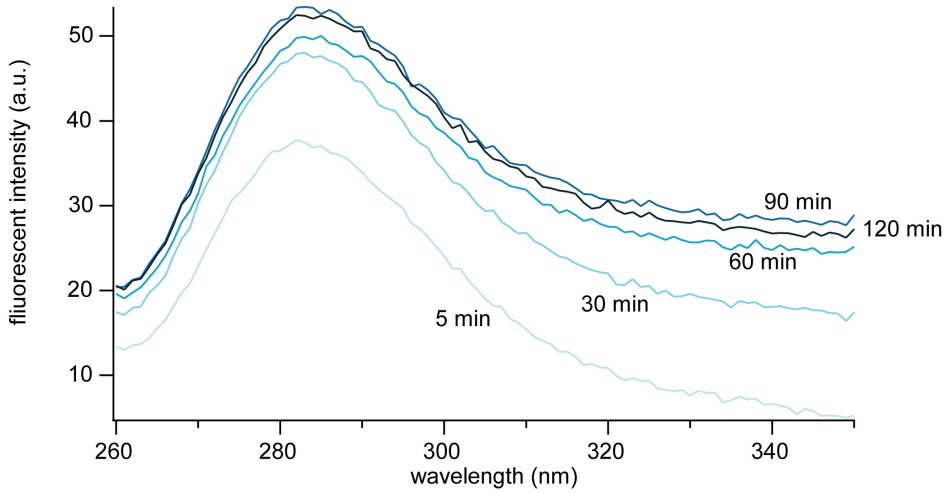

Supplementary Figure 10 | UV fluorescence spectroscopy detection of fMLP released from PLGA beads. The excitation wavelength was 240 nm and the fluorescence emission spectrum was recorded in the range from 260 nm to 350 nm. The peak region of this spectrum around 284 nm was used for the quantification of the concentration of fMLP at various time points of release.

Nature Methods: doi:10.1038/nmeth.1400

Supplementary Note 1

Controlled release of encapsulated agents

Diffusion controls the shape of the concentration profile of molecules released from a microsource in a quiescent solution. In steady state and for spherical symmetry, the diffusion equation reduces to $\nabla^2 c(r) = 0$, where c is the concentration. The solution of this equation for a particle with radius a is

$$c(r) = c_0 \cdot \frac{a}{r}, \qquad \textbf{Supplementary Equation 1}$$

where c_0 is the concentration at the surface ($r = a$) of the particle. This accurately describes the concentration profile around an isolated bead. However in our experiments we stimulate cells adherent to a coverslip which blocks the diffusion of free molecules, thereby modifying the concentration profile. This barrier can be taken into account by using the "method of images": The concentration profile around a single bead at a height h above a coverslip can be approximated by adding the concentration profile of an imaginary bead located at a height h below the coverslip to the concentration profile of the real bead located at a height h above the coverslip (Equation 1 in the article). The resulting distribution for a hypothetical $h = 3 \cdot a$ is shown in **Supplementary Figure 2a.**

Fick's first law of diffusion relates concentration gradients and molecular fluxes. The concentration of released molecules at the surface of a microsource c_0 is therefore related to the flux of molecules from the surface j_0 and their diffusion coefficient D:

$$c_0 = j_0 \cdot \frac{a}{D}. \qquad \textbf{Supplementary Equation 2}$$

To estimate the flux from individual beads, we measured the release of fMLP from ensembles of PLGA beads with two complementary methods: high performance liquid chromatography (HPLC) and ultraviolet fluorescence spectroscopy (UV spectroscopy). **Supplementary Figure 2b** shows the time course of fMLP released from PLGA beads within the first three hours after suspending the beads in aqueous solution. Both HPLC and UV spectroscopy measurements yield essentially the same results: Beads at a concentration of 1 mg/ml release 60 μM of fMLP during the first hour. The release rate seems to scale linearly with the nominal loading. As described in the main part of the article, the resulting fMLP concentration on the surface of a bead with a diameter of 2 μm is therefore c_0 = 8 nM (**Supplementary Fig. 2a**).

Nature Methods: doi:10.1038/nmeth.1400

Supplementary Note 2

Particle size dependence of release rate

We investigated how the release rate of beads (number of molecules released per time) depends on their size by measuring the release of molecules from individual PLGA microsources. We used confocal microscopy to image the residual fluorescence in beads releasing the fluorescent dye rhodamine B. The residual fluorescence of individual beads was quantified by integrating background-subtracted z-stacks of images acquired with a 100x oil immersion lens with a numerical aperture of 1.40 on a spinning disk confocal microscope. We minimized the influence of bleaching by minimizing the light exposure and using a highly sensitive cooled EM-CCD camera (Andor iXon DU 897). We measured the release curves with different light exposure levels which varied by a factor of up to 10 and found that the release curves do not dependent on the exposure level. This indicates that bleaching of the dye is negligible. The results of these measurements show that the release rate scales approximately with the volume of the particle (**Supplementary Fig. 3**).

Nature Methods: doi:10.1038/nmeth.1400

Supplementary Note 3

Bulk cell response to chemoattractants released from beads

We tested whether the fMLP encapsulated into and released from the beads is able to induce a chemotactic response in neutrophils. A Zigmond diffusion chamber was used to create gradients of released fMLP and the migration of HL-60 neutrophils in the chamber was measured.

We suspended fMLP-loaded PLGA beads in buffer solution and let them release fMLP for a defined amount of time (30 or 60 minutes). Afterwards, we spun down the beads and collected the supernatant containing the released fMLP. Based on the release measurements shown in **Supplementary Figure 2b**, we calculated how much the supernatant had to be diluted to reach final concentrations of fMLP on the order of about 10-100 nM. The Zigmond chamber was filled with released fMLP in one reservoir of the chamber and with control buffer in the other reservoir. The cell migration was measured by phase contrast microscopy. We found good chemotaxis response (**Supplementary Fig. 4**) when we used the released fMLP at concentrations between 30 nM and 130 nM. In control measurements (data not shown), we used fMLP directly (not loaded into PLGA beads and then released from PLGA beads) in Zigmond chambers and we found that we get good chemotaxis response if we use fMLP at concentrations of about 50 nM. This indicates that the potency of fMLP to stimulate chemotaxis is not reduced if it is loaded into and then released from PLGA beads. Furthermore, this result also verifies the quantification of the fMLP release from the beads as shown in **Supplementary Figure 2b**.

Nature Methods: doi:10.1038/nmeth.1400

Supplementary Note 4

Temporal flexibility

The dynamic reconfiguration of optical traps provides a high degree of temporal flexibility. Care must be taken when moving microsources rapidly. It can be shown[1], that the steady state solution (**Supplementary Equation 1 in Supplementary Note 1**) is a good approximation for the concentration distribution in the region of interest $r \leq r_s$ around the bead provided that the velocity v of the bead is small enough: $v << 2D\, r_s^{-1}$. For $r_s = 30\ \mu m$, this condition is fulfilled if $v << 70\ \mu m\ s^{-1}$. Given that the particle velocity in our experiments was about $v = 1\ \mu m\ s^{-1}$ we can consider the concentration distribution around the bead to be always in steady state. After a fast rearrangement, the concentration distribution will need time to relax[2]. The steady state distribution in the region $r \leq r_s$ is reached after a time $t \gg t_s$ where $t_s = r_s^2\ (4\ D)^{-1}$. In the case presented here, for a $r_s = 30\ \mu m$ region of interest around the beads, we find a relaxation time of $t_s = 0.23\ s$. Therefore it is possible to switch between well defined spatial stimulation patterns on length scales of several tens of micrometers within about one second.

In addition to using multiple beads in order to create flexible *spatial* stimulation patterns, flexible *temporal* stimulation patterns can be applied to a cell by dynamically changing the distance between one or more beads and the cell. The maximal frequency f_m of stimulation that can be transmitted by the diffusing chemicals over the distance r_s is approximately the inverse of the relaxation time $f_m = t_s^{-1} = 4D\, r_s^{-2}$. Therefore a frequency of 30 Hz (the maximal frequency of stimulation that can be created by our current implementation of holographic optical tweezers) can be transmitted over a range of 12 µm.

Nature Methods: doi:10.1038/nmeth.1400

Supplementary Note 5

Influence of cell onto concentration pattern

We investigated how the presence of cells affects concentration patterns of fMLP around microsources. We performed 3D stochastic simulations of a bead releasing molecules in close vicinity to the leading edge of a cell (**Supplementary Fig. 6**). The simulated bead had a diameter of 2 µm and a surface-to-surface distance of 0.5 µm to the coverslip and provided a constant release of freely diffusing molecules. Lamellipodia at the leading edges of cells such as neutrophils have typically a thickness of about 0.1 - 0.2 µm and the thickness of the cells increases with decreasing distance to the cell center. We approximated the leading edge of the simulated cell by a disc with a height of 0.5 µm and a radius of 10 µm. The results of these simulations are shown in **Supplementary Figure 6b-d**. It can be seen that the concentration profile around the bead is not perturbed significantly by the presence of a purely repulsive cell.

In the opposite extreme, the cells could also act as perfect sinks. This has a larger effect on the concentration profile – indeed it would go to zero at a perfectly absorbing surface. However, since fMLP binding sites cover only a very small fraction of the surface, we expect that the purely repulsive limit is a much better approximation. The sizes of the fMLP receptors and their surface density are known to be about 24-95 kDa[3] and on the order of 100,000 receptors per cell[4]. Thus the surface coverage of binding sites is less than about 1%.

Nature Methods: doi:10.1038/nmeth.1400

Supplementary Note 6

Heating of the trapped particle due to the trapping laser

We used the temperature-dependent fluorescent dye Rhodamine B to quantify the heating of PLGA particles due to the trapping laser. The intensity of the fluorescence emitted from Rhodamine B decreases by 2.3% per 1ºC temperature increase[5]. We suspended PLGA particles in a solution of 0.05 mM Rhodamine B. Single particles on coverslips in optical traps and their surrounding were imaged with spinning disk confocal microscopy. Images were taken at a maximal laser power of about 230 mW in the focal plane and also at 0 mW laser power. The temperature distribution around a particle in a trap was derived from the ratio between an image at high laser power and at zero power. The temperature distribution around a particle with a diameter of 2.7 μm is shown in **Supplementary Figure 7a**. Line profiles of this distribution in x- and y-direction are shown in red in **Supplementary Figure 7b,c**. The direct vicinity of the particle is heated up by ΔT with respect to the background room temperature T_0. The temperature $T(r)$ decreases with increasing distance r from a bead with a radius a

$$T(r) = T_0 + \Delta T \cdot \frac{a}{r}$$

Fits of this function to the four line profiles are also shown in **Supplementary Figure 7b,c**. The fits had the bead radius a = 1.35 μm as fixed parameter and T_0 and ΔT as fit parameters. The temperature increase at the bead surface was found to be $\Delta T = 4.3 \pm 0.5$ ºC. This yields a temperature increase of 19 ± 2 ºC W^{-1} for a PLGA particle with a diameter of 2.7 μm. The trapping powers used in the cell stimulation experiments were about 5 mW. Therefore, the corresponding temperature increase of trapped particles of a similar size is about 0.09 ± 0.01 ºC. Since control particles that were not releasing fMLP or cytochalasin D (CD) did not affect the cell behaviour, this temperature increase is considered as negligible for this study.

Nature Methods: doi:10.1038/nmeth.1400

Supplementary Note 7

Factors influencing the concentrations on the bead surface

Controlled release particles contain a finite amount of loaded molecules. Conservation of mass and the experimental time scales limit the flux of released molecules. However, as long as the time that a particle releases molecules is larger than the typical time that an experiment takes, this does not impose a serious obstacle. In the examples shown here this condition is fulfilled if the experiment does not take much longer than an hour. PLGA controlled release systems show a strong rapid initial release ("initial burst") and a slow release period that can lasts for days or weeks ("lag-time")[6]. Exploiting this slow long-lasting release period increases the time that is available for experiments by several orders of magnitude. However, as the release is slowed down, the concentration of stimulant decreases. For a constant flux of molecules from a particle, the diffusion of the released molecules determines the resulting concentration profiles around the particles. In general, the concentration c_0 of the molecule at the surface of the spherical particle is

$$c_0 = \frac{l \cdot \rho_b \cdot a^2}{3 \cdot M_w \cdot t_r \cdot D}$$

where l is the loading ratio (mass of molecules that are loaded into the particle divided by mass of particle), which is considered to be small compared to 1, ρ_b is the mass density of the particle material, a is the radius of the particle, M_w is the molecular weight of the molecule, t_r is the release time (time that it takes for total release after the bead is put into solution) and D is the diffusion coefficient of the molecule (please note that a and t_r are not necessarily independent of each other). For example, concentrations of up several hundred nM could be achieved for particles with diameter on the order of about 10 µm with a release time of 10 hours.

Nature Methods: doi:10.1038/nmeth.1400

LITERATURE

1 Leal, L. G. *Advanced Transport Phenomena*. (Cambridge University Press, 2007).

2 Berg, H. C. *Random Walks in Biology*. (Princeton University Press, 1993).

3 De Nardin, E., Radel, S. J. & Genco, R. J. Isolation and partial characterization of the formyl peptide receptor components on human neutrophils. *Biochemical and Biophysical Research Communications* **174**, 84-89 (1991).

4 Andreoli, T. E. *et al. Molecular Biology of Membrane Transport Disorders*. 2nd edn, (Springer, 1996).

5 Ebert, S., Travis, K., Lincoln, B. & Guck, J. Fluorescence ratio thermometry in a microfluidic dual-beam laser trap. *Optics Express* **15**, 15493-15499 (2007).

6 Wang, J., Wang, B. A. & Schwendeman, S. P. Characterization of the initial burst release of a model peptide from poly(D,L-lactide-co-glycolide) microspheres. *Journal of Controlled Release* **82**, 289-307 (2002).

Nature Methods: doi:10.1038/nmeth.1400